Acta Cryst E CRYSTALLOGRAPHIC COMMUNICATIONS

ISSN 2056-9890

Synthesis, crystal structure, Hirshfeld surface and crystal void analysis of 4-fluorobenzo[*c*][1,2,5]-selenadiazol-1-ium chloride

Atash V. Gurbanov,[a] Tuncer Hökelek,[b] Gunay Z. Mammadova,[c] Khudayar I. Hasanov,[d] Tahir A. Javadzade[e] and Alebel N. Belay[f]*

[a]Excellence Center, Baku State University, Z. Xalilov Str. 23, Az 1148 Baku, Azerbaijan, [b]Hacettepe University, Department of Physics, 06800 Beytepe-Ankara, Türkiye, [c]Department of Chemistry, Baku State University, Z. Khalilov Str. 23, Az 1148 Baku, Azerbaijan, [d]Azerbaijan Medical University, Scientific Research Centre (SRC), A. Kasumzade Str. 14, AZ 1022 Baku, Azerbaijan, [e]Department of Chemistry and Chemical Engineering, Khazar University, Mahzati Str. 41, AZ 1096 Baku, Azerbaijan, and [f]Department of Chemistry, Bahir Dar University, PO Box 79, Bahir Dar, Ethiopia. *Correspondence e-mail: alebel.nibret@bdu.edu.et

Received 6 January 2025
Accepted 14 February 2025

Edited by M. Weil, Vienna University of Technology, Austria

Keywords: crystal structure; non-covalent interactions; chalcogen bond; organic–inorganic salt.

CCDC reference: 2424642

Supporting information: this article has supporting information at journals.iucr.org/e

The asymmetric unit of the title salt, $C_6H_4FN_2Se^+\cdot Cl^-$, contains one planar 4-fluorobenzo[*c*][1,2,5]selenadiazol-1-ium molecular cation and a chloride anion. In the crystal, intermolecular N—H···Cl hydrogen bonds link the 4-fluorobenzo[*c*][1,2,5]selenadiazol-1-ium molecules, which are arranged in parallel layers along (104), to the chloride anions. The cationic layers, in turn, are stacked along [001]. A Hirshfeld surface analysis of the crystal structure indicates that the most important contributions for the crystal packing are from H···Cl/Cl···H (22.6%), H···F/F···H (13.9%), H···N/N···H (11.9%), H···C/C···H (10.2%) and H···H (7.7%) interactions. The volume of the crystal voids and the percentage of free space were calculated to be 44.80 Å^3 and 5.91%, showing that there is no large cavity in the crystal packing.

1. Chemical context

Replacement of the H atom at the *R*—H···Nu synthon (Nu = nucleophile) with a group 16 element can lead to the formation of a chalcogen bond (ChB), which is a non-covalent interaction between the electron-density-deficient side (so-called σ- or π-hole) of a covalently bonded chalcogen atom (Ch = O, S, Se or Te) and a nucleophilic (Nu) region in the same (intramolecular) or another (intermolecular) molecular entity so that *R*—Ch···Nu [*R* = Ch, Pn (pnictogen), metal, *etc.*; Nu = lone pair possessing Ha (halogen), Ch, Pn or metal atom, anion, π-system, radical, etc.] can be formed (Aliyeva *et al.*, 2024). Similarly to hydrogen, halogen or pnictogen bonds, as well as to π-interactions (Abdelhamid *et al.*, 2011; Gurbanov *et al.*, 2018), the chalcogen bond is also of importance for the development of new catalysts based on metal complexes, or sensors, molecular switches, *etc.* Following the concept of resonance-assisted hydrogen bonds (Maharramov *et al.*, 2010; Mahmudov *et al.*, 2011), a resonance-assisted chalcogen bond is usually treated as a chalcogen bond strengthened by conjugation in a π-system due to electron (charge) delocalization or favourable rearrangement of charge distribution in the molecular system (Gurbanov *et al.*, 2020). Like charge-assisted hydrogen bonds (Mac Leod *et al.*, 2012; Martins *et al.*, 2017; Mizar *et al.*, 2012), the Ch···Nu bond can be strengthened by using an anion instead of traditional nucleophiles bearing a lone pair, which may lead to charge-assisted chalcogen-bonding (Guseinov *et al.*, 2022).

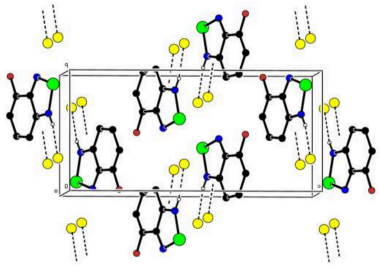

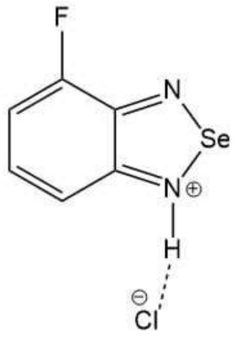

In the context given above, we have isolated the charge-assisted and chalcogen-bonded title salt, $(C_6H_4FN_2Se)^+Cl^-$, and studied its molecular and crystal structures together with a Hirshfeld surface and crystal voids analysis.

2. Structural commentary

The asymmetric unit of the title compound contains one 4-fluorobenzo[c][1,2,5]selenadiazol-1-ium cationic molecule and a chloride anion (Fig. 1). The 4-fluorobenzo[c][1,2,5]selenadiazol-1-ium molecule is almost planar, where the planar *A* (C1–C6) and *B* (Se/N1/N2/C1/C2) rings are oriented at a dihedral angle of *A*/*B* = 0.64 (6)°. Atom F1 is 0.0063 (18) Å out of the least-squares plane of ring *A*. All bond lengths and angles in the molecule are normal.

3. Supramolecular features

In the crystal, intermolecular N—H···Cl hydrogen bonds link the molecular cations, which are arranged into parallel layers along (104), and chloride ions (Table 1). The cationic layers, in turn, are stacked along [001 (Fig. 2*a*). The closest Se···Cl separations of 2.883 (2) and 3.030 (2) Å are shorter than the sum of the van der Waals radii (ΣrvdW (Se···Cl) = 3.65 Å) and therefore can be considered as charge-assisted chalcogen bonds, which aggregate the title compound into a supramolecular dimer, with the σ-hole angles ∠N1—Se1···Cl1 and ∠N1—Se1···Cl1 of 171.69 (7)° and 177.19 (7)° (Fig. 2*b*). Neither π–π nor C—H···π(ring) interactions are observed.

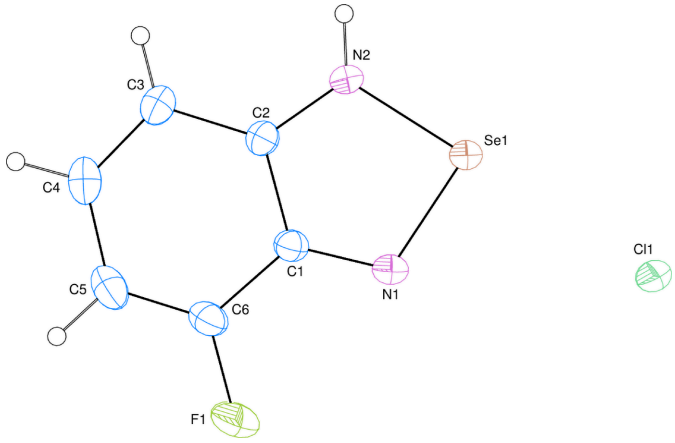

Figure 1
The asymmetric unit of the title compound with displacement ellipsoids drawn at the 50% probability level.

Table 1
Hydrogen-bond geometry (Å, °).

D—H···*A*	*D*—H	H···*A*	*D*···*A*	*D*—H···*A*
N2—H2*N*···Cl1^{i}	0.85	2.23	3.056 (3)	163

Symmetry code: (i) $x, y+1, z$.

4. Hirshfeld surface analysis

A Hirshfeld surface (HS) analysis (Hirshfeld, 1977; Spackman & Jayatilaka, 2009) was carried out to visualize the intermolecular interactions in the crystal of the title compound using *CrystalExplorer* (Spackman *et al.*, 2021). In the three-dimensional Hirshfeld surface plotted over d_{norm} (Fig. 3*a*), the contact distances equal to the sum of van der Waals radii are shown by the white surfaces, whereas distances shorter and longer than the van der Waals radii are shown in red and blue, respectively (Venkatesan *et al.*, 2016), where the bright-red spots indicate their roles as the respective donors and/or acceptors. Planar stacking arrangements and the presence of aromatic stacking interactions such as C—H···π and π–π interactions are visualized by shape-index. In the HS plotted over shape-index, the C—H···π interactions are represented

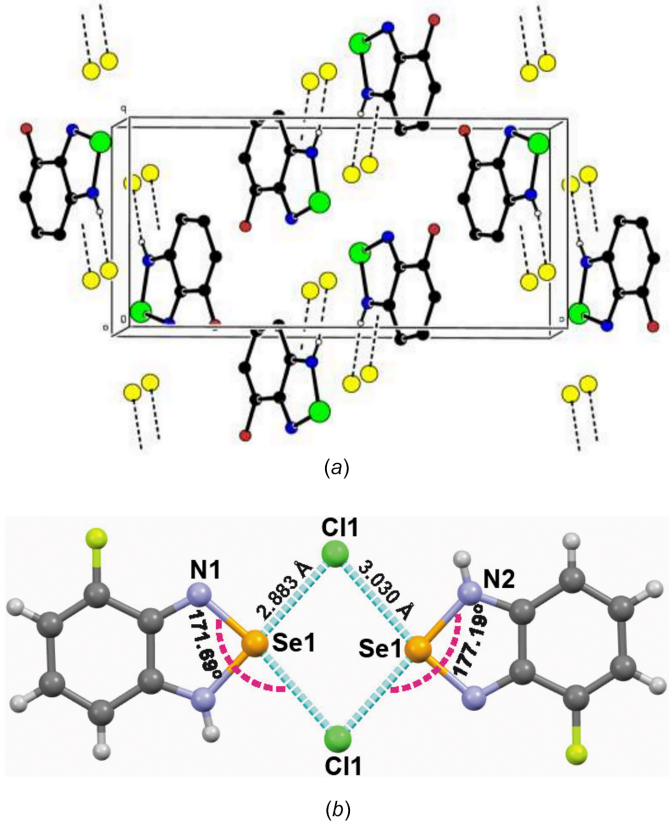

Figure 2
(*a*) Crystal packing diagram viewed down the *a* axis with intermolecular N—H···Cl hydrogen bonds shown as dashed lines; (*b*) intermolecular charge-assisted chalcogen bonds shown as dashed blue lines.

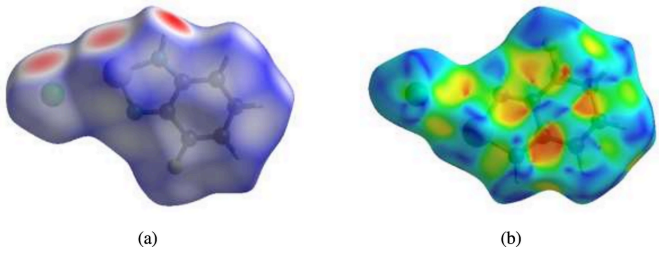

Figure 3
(*a*) View of the three-dimensional Hirshfeld surface of the title compound plotted over d_{norm} and (*b*) Hirshfeld surface of the title compound plotted over shape-index.

as red π-holes, which are related to the electron ring interactions between the CH groups with the centroid of the aromatic rings of neighbouring molecules. On the other hand, π–π stacking interactions are visualized by the presence of adjacent red and blue triangles. Fig. 3*b* clearly suggests that there are neither C—H$\cdots\pi$ nor π–π interactions present.

The overall two-dimensional fingerprint plot, Fig. 4*a*, and those delineated into H$\cdots$Cl/Cl$\cdots$H, H$\cdots$F/F$\cdots$H, H$\cdots$N/N$\cdots$H, H$\cdots$C/C$\cdots$H, H$\cdots$H, C$\cdots$Cl/Cl$\cdots$C, Cl$\cdots$Se/Se$\cdots$Cl, F$\cdots$Se/Se$\cdots$F, H$\cdots$Se/Se$\cdots$H, F$\cdots$C/C$\cdots$F, C$\cdots$N/N$\cdots$C, N$\cdots$Se/Se$\cdots$N, C$\cdots$Se/Se$\cdots$C, F$\cdots$Cl/Cl$\cdots$F, N$\cdots$N, C$\cdots$C, Se$\cdots$Se and F$\cdots$N/N$\cdots$F (McKinnon *et al.*, 2007) are illustrated in Fig. 4*b–s*, respectively, together with their relative contributions to the Hirshfeld surface. The most important interaction is H$\cdots$Cl/Cl$\cdots$H (Fig. 4*b*), contributing 22.6% to the HS, and viewed as a pair of spikes at $d_e + d_i$ = 2.06 Å. The H$\cdots$F/F$\cdots$H (Table 2 and Fig. 4*c*) and H$\cdots$N/N$\cdots$H (Fig. 4*d*) contacts contribute 13.9% and 11.9%, respectively, to the HS and are viewed as pairs of spikes at $d_e + d_i$ = 2.42 Å and $d_e + d_i$ = 2.72 Å, respectively. In the absence of C—H$\cdots\pi$ interactions, the H$\cdots$C/C$\cdots$H contacts (Fig. 4*e*), contributing 10.2% to the HS, are reflected at $d_e + d_i$ = 3.28 Å. The H$\cdots$H interactions (Fig. 4*f*) contribute 7.7% to the HS, and are viewed at $d_e = d_i$ = 1.22 Å. The C$\cdots$Cl/Cl$\cdots$C contacts (Fig. 4*g*) with a 6.3% contribution to the HS, have an arrow-shaped distribution of points, and they are viewed at $d_e = d_i$ = 1.84 Å. The pair of spikes of the Cl$\cdots$Se/Se$\cdots$Cl contacts (Fig. 4*h*) with 5.4% contribution to the HS are seen at $d_e + d_i$ = 3.00 Å. Finally, the F$\cdots$Se/Se$\cdots$F (Fig. 4*i*), H$\cdots$Se/Se$\cdots$H (Fig. 4*j*), F$\cdots$C/C$\cdots$F (Fig. 4*k*), C$\cdots$N/N$\cdots$C (Fig. 4*l*), N$\cdots$Se/Se$\cdots$N (Fig. 4*m*), C$\cdots$Se/Se$\cdots$C (Fig. 4*n*), F$\cdots$Cl/Cl$\cdots$F (Fig. 4*o*), N$\cdots$N (Fig. 4*p*), C$\cdots$C (Fig. 4*q*), Se$\cdots$Se (Fig. 4*r*) and F$\cdots$N/N$\cdots$F (Fig. 4*s*) contacts with 3.9%, 3.7%, 3.4%, 3.4%, 2.1%, 1.4%, 1.2%, 1.1%, 1.1%, 0.5% ad 0.2% contributions, respectively, to the HS make very small contributions.

Table 2
Selected interatomic distances (Å).

N2$\cdots$Cl1^{i}	3.056 (3)	F1$\cdots$N1	2.800 (3)
H2*N*$\cdots$Cl1^{i}	2.23	H5$\cdots$F1^{ii}	2.56

Symmetry codes: (i) $x, y+1, z$; (ii) $-x+2, y+\frac{1}{2}, -z+\frac{1}{2}$.

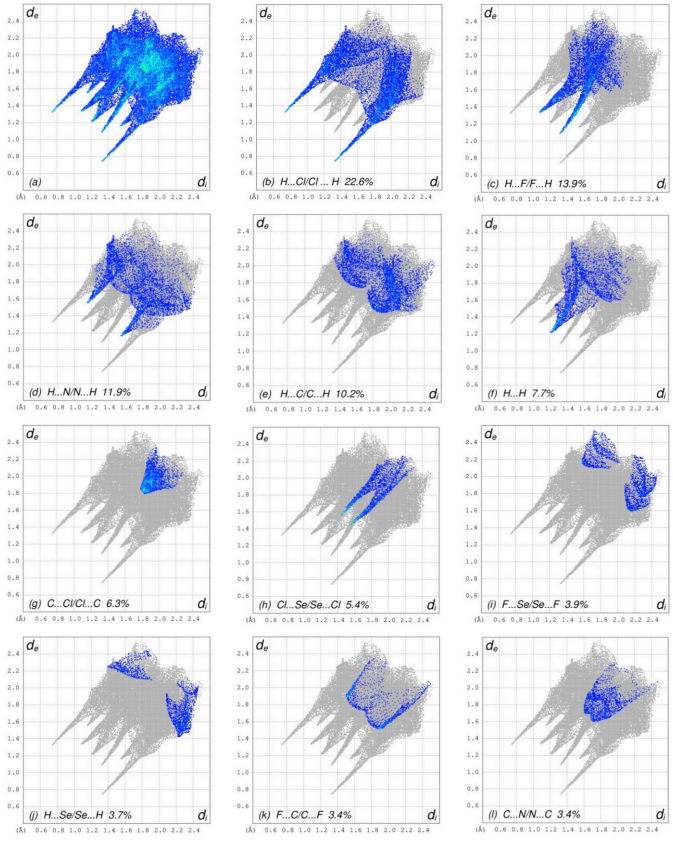

Figure 4
The full two-dimensional fingerprint plots for the title compound, showing (*a*) all interactions, and delineated into (*b*) H$\cdots$Cl/Cl$\cdots$H, (*c*) H$\cdots$F/F$\cdots$H, (*d*) H$\cdots$N/N$\cdots$H, (*e*) H$\cdots$C/C$\cdots$H, (*f*) H$\cdots$H, (*g*) C$\cdots$Cl/Cl$\cdots$C, (*h*) Cl$\cdots$Se/Se$\cdots$Cl, (i) F$\cdots$Se/Se$\cdots$F, (*j*) H$\cdots$Se/Se$\cdots$H, (*k*) F$\cdots$C/C$\cdots$F, (*l*) C$\cdots$N/N$\cdots$C, (*m*) N$\cdots$Se/Se$\cdots$N, (*n*) C$\cdots$Se/Se$\cdots$C, (*o*) F$\cdots$Cl/Cl$\cdots$F, (*p*) N$\cdots$N, (*q*) C$\cdots$C, (*r*) Se$\cdots$Se and (*s*) F$\cdots$N/N$\cdots$F interactions. The d_i and d_e values are the closest internal and external distances (in Å) from given points on the Hirshfeld surface.

The nearest neighbour coordination environment of a molecule can be determined from the colour patches on the HS based on how close to other molecules they are. The HS

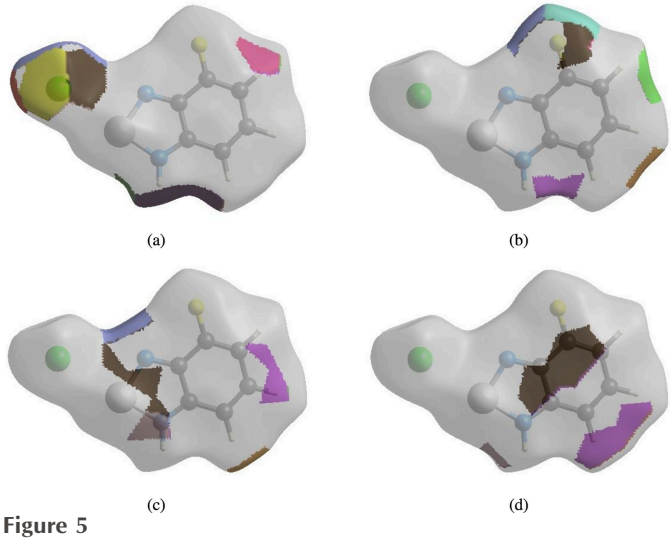

Figure 5
The Hirshfeld surface representations with the function d_{norm} plotted onto the surface for (*a*) H$\cdots$Cl/Cl$\cdots$H, (*b*) H$\cdots$F/F$\cdots$H, (*c*) H$\cdots$N/N$\cdots$H and (*d*) H$\cdots$C/C$\cdots$H interactions.

representations of contact patches plotted onto the surface are shown for the H···Cl/Cl···H, H···F/F···H, H···N/N···H and H···C/C···H interactions in Fig. 5*a–d*.

The Hirshfeld surface analysis confirms the importance of H-atom contacts in establishing the packing. The large number of H···Cl/Cl···H, H···F/F···H, H···N/N···H and H···C/C···H interactions suggest that van der Waals interactions and hydrogen bonding play the major roles in the crystal packing (Hathwar *et al.*, 2015).

5. Crystal voids

If the crystal packing does not result in significant voids, then the molecules are tightly packed and the applied external mechanical force may not easily break the crystal. Thus, the strength of the crystal packing is important for determining the response to an applied mechanical force. To check the mechanical stability of the crystal, a void analysis was performed by adding up the electron densities of the spherically symmetric atoms contained in the asymmetric unit (Turner *et al.*, 2011; Irrou *et al.*, 2022). The volume of the crystal voids (Fig. 6*a*,*b*) and the percentage of free space in the unit cell were calculated to be 44.80 Å^3 and 5.91%, respectively. Thus, the crystal packing appears compact and the mechanical stability should be substantial.

6. Database survey

A survey of the Cambridge Structural Database (CSD; version 5.45, update of September 2024; Groom *et al.*, 2016) found two molecules that are similar to the title compound, *viz.* (*rac*)-4-methyl-4-nitro-2,1,3-benzoselena-diazol-5(4*H*)-one, $C_7H_5N_3O_3Se$ (CSD refcode JURLAJ; Tian *et al.*, 1993) and 5-nitro-2,1,3-benzoselenadiazole, $C_6H_3N_3O_2Se$ (CSD refcode DOBWUO; Aliyeva *et al.*, 2024). In contrast to the four-membered Se_2Cl_2 ring defined through charge-assisted chalcogen bonds in the crystal packing of the title compound, there is an Se_2N_2 supramolecular synthon with intermolecular chalcogen bonds in JURLAJ and DOBWUO.

Table 3
Experimental details.

Crystal data	
Chemical formula	$C_6H_4FN_2Se^+\cdot Cl^-$
M_r	237.52
Crystal system, space group	Monoclinic, $P2_1/c$
Temperature (K)	296
a, b, c (Å)	6.889 (4), 7.250 (5), 15.183 (10)
β (°)	90.90 (3)
V (Å^3)	758.2 (9)
Z	4
Radiation type	Mo $K\alpha$
μ (mm^{-1})	5.25
Crystal size (mm)	0.34 × 0.23 × 0.14
Data collection	
Diffractometer	Bruker APEXII CCD
Absorption correction	Multi-scan (*SADABS*; Krause *et al.*, 2015)
T_{min}, T_{max}	0.252, 0.498
No. of measured, independent and observed [$I > 2\sigma(I)$] reflections	9806, 1768, 1528
R_{int}	0.046
(sin $\theta/\lambda)_{max}$ (Å^{-1})	0.658
Refinement	
$R[F^2 > 2\sigma(F^2)]$, $wR(F^2)$, S	0.025, 0.055, 1.07
No. of reflections	1768
No. of parameters	100
H-atom treatment	H-atom parameters constrained
$\Delta\rho_{max}$, $\Delta\rho_{min}$ (e Å^{-3})	0.27, −0.41

Computer programs: *APEX4* and *SAINT* (Bruker, 2020), *SHELXT2019/1* (Sheldrick, 2015*a*), *SHELXL2019/1* (Sheldrick, 2015*b*), *SHELXTL* (Sheldrick, 2008) and *publCIF* (Westrip, 2010).

7. Synthesis and crystallization

3-Fluorobenzene-1,2-diamine (10 mmol) and selenium dioxide (10 mmol) were dissolved in 25 ml of dichloromethane

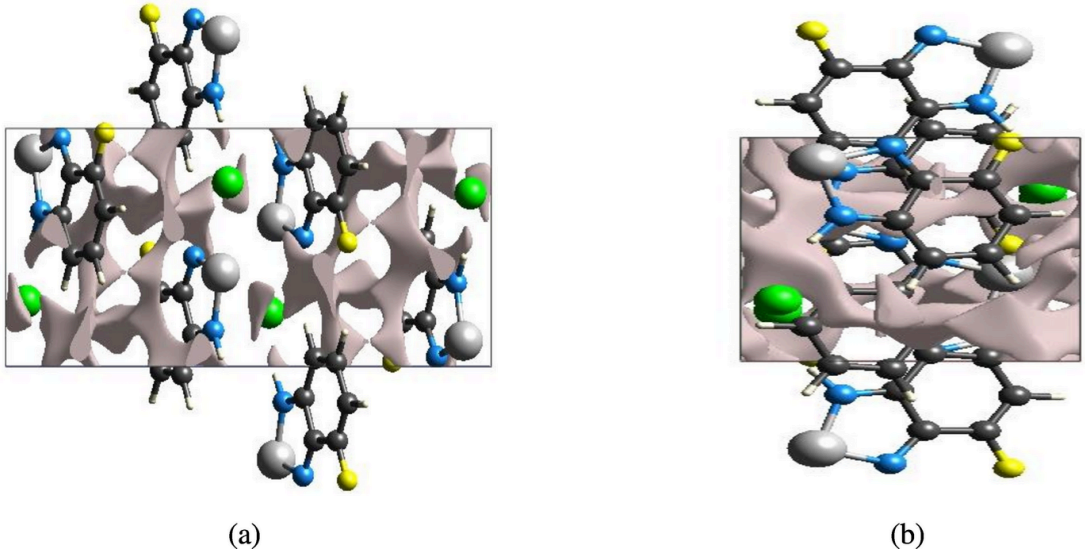

Figure 6
Graphical views of voids in the crystal packing of the title compound (*a*) along the *a* axis and (*b*) along the *b* axis.

and stirred for 1 h at ambient temperature, and further refluxed for 1 h. After cooling to room temperature, the solvent was evaporated under reduced pressure to give the reaction product. The title compound was obtained by slow evaporation of a water–acetone (1:3 *v*:*v*) solution of the reaction product at pH = 2 (adjusted by addition of HCl), and analysed by single-crystal X-ray analysis, elemental analysis, ESI-MS and NMR measurements. Yield: 87% (based on SeO_2), yellow powder soluble in methanol, ethanol and DMSO. Analysis calculated for $C_6H_4ClFN_2Se$ (M_r = 237.53): C, 30.34; H, 1.70; N, 11.79. Found: C, 30.29; H, 1.67; N, 11.76. ESI-MS (positive ion mode), *m*/*z*: 238.4 $[M + H]^{+\cdot}$ ^{1}H NMR ($CDCl_3$), δ: 6.77–7.92 (3H, Ar–H). ^{13}C NMR ($CDCl_3$), 110.91, 119.58, 128.96, 151.29, 155.67 and 161.93.

8. Refinement

Crystal data, data collection and structure refinement details are summarized in Table 3. The N- and C-bond hydrogen atom positions were calculated geometrically at distances of 0.85 Å and 0.93 Å (for aromatic CH) and refined using a riding model by applying the constraint of $U_{iso}(H) = 1.2U_{eq}(C, N)$.

Acknowledgements

The author's contributions are as follows. Conceptualization, AVG, TH and ANB; synthesis, AVG and GZM; X-ray analysis, AVG; writing (review and editing of the manuscript) AVG and TH; funding acquisition, AVG, GZM, KIH and TAJ; supervision, AVG, TH and ANB.

Funding information

This work has been supported by Baku State University, Azerbaijan Medical University and Khazar University in Azerbaijan. TH is also grateful to Hacettepe University Scientific Research Project Unit (grant No. 013 D04 602 004).

References

Abdelhamid, A. A., Mohamed, S. K., Khalilov, A. N., Gurbanov, A. V. & Ng, S. W. (2011). *Acta Cryst.* E**67**, o744.
Aliyeva, V. A., Gurbanov, A. V., Guedes da Silva, M. F. C., Gomila, R. M., Frontera, A., Mahmudov, K. T. & Pombeiro, A. J. L. (2024). *Cryst. Growth Des.* **24**, 781–791.
Bruker (2020). *APEX4* and *SAINT*. Bruker AXS, Madison, Wisconsin, USA.
Groom, C. R., Bruno, I. J., Lightfoot, M. P. & Ward, S. C. (2016). *Acta Cryst.* B**72**, 171–179.
Gurbanov, A. V., Kuznetsov, M. L., Mahmudov, K. T., Pombeiro, A. J. L. & Resnati, G. (2020). *Chem. A Eur. J.* **26**, 14833–14837.
Gurbanov, A. V., Maharramov, A. M., Zubkov, F. I., Saifutdinov, A. M. & Guseinov, F. I. (2018). *Aust. J. Chem.* **71**, 190–194.
Guseinov, F. I., Malinnikov, V. M., Lialin, K. N., Kobrakov, K. I., Shuvalova, E. V., Nelyubina, Y. V., Ugrak, B. I., Kustov, L. M. & Mahmudov, K. T. (2022). *Dyes Pigments*, **197**, 109898.
Hathwar, V. R., Sist, M., Jørgensen, M. R. V., Mamakhel, A. H., Wang, X., Hoffmann, C. M., Sugimoto, K., Overgaard, J. & Iversen, B. B. (2015). *IUCrJ*, **2**, 563–574.
Hirshfeld, H. L. (1977). *Theor. Chim. Acta*, **44**, 129–138.
Irrou, E., Elmachkouri, Y. A., Oubella, A., Ouchtak, H., Dalbouha, S., Mague, J. T., Hökelek, T., El Ghayati, L., Sebbar, N. K. & Taha, M. L. (2022). *Acta Cryst.* E**78**, 953–960.
Krause, L., Herbst-Irmer, R., Sheldrick, G. M. & Stalke, D. (2015). *J. Appl. Cryst.* **48**, 3–10.
Mac Leod, T. C. O., Kopylovich, M. N., Guedes da Silva, M. F. C., Mahmudov, K. T. & Pombeiro, A. J. L. (2012). *Appl. Catal. Gen.* **439–440**, 15–23.
Maharramov, A. M., Aliyeva, R. A., Aliyev, I. A., Pashaev, F. H., Gasanov, A. G., Azimova, S. I., Askerov, R. K., Kurbanov, A. V. & Mahmudov, K. T. (2010). *Dyes Pigments*, **85**, 1–6.
Mahmudov, K. T., Maharramov, A. M., Aliyeva, R. A., Aliyev, I. A., Askerov, R. K., Batmaz, R., Kopylovich, M. N. & Pombeiro, A. J. L. (2011). *J. Photochem. Photobiol. Chem.* **219**, 159–165.
Martins, N. M. R., Anbu, S., Mahmudov, K. T., Ravishankaran, R., Guedes da Silva, M. F. C., Martins, L. M. D. R. S., Karande, A. A. & Pombeiro, A. J. L. (2017). *New J. Chem.* **41**, 4076–4086.
McKinnon, J. J., Jayatilaka, D. & Spackman, M. A. (2007). *Chem. Commun.* pp. 3814–3816.
Mizar, A., Guedes da Silva, M. F. C., Kopylovich, M. N., Mukherjee, S., Mahmudov, K. T. & Pombeiro, A. J. L. (2012). *Eur. J. Inorg. Chem.* pp. 2305–2313.
Sheldrick, G. M. (2008). *Acta Cryst.* A**64**, 112–122.
Sheldrick, G. M. (2015*a*). *Acta Cryst.* A**71**, 3–8.
Sheldrick, G. M. (2015*b*). *Acta Cryst.* C**71**, 3–8.
Spackman, M. A. & Jayatilaka, D. (2009). *CrystEngComm*, **11**, 19–32.
Spackman, P. R., Turner, M. J., McKinnon, J. J., Wolff, S. K., Grimwood, D. J., Jayatilaka, D. & Spackman, M. A. (2021). *J. Appl. Cryst.* **54**, 1006–1011.
Tian, W., Grivas, S. & Olsson, K. (1993). *J. Chem. Soc. Perkin Trans. 1*, pp. 257–261.
Turner, M. J., McKinnon, J. J., Jayatilaka, D. & Spackman, M. A. (2011). *CrystEngComm*, **13**, 1804–1813.
Venkatesan, P., Thamotharan, S., Ilangovan, A., Liang, H. & Sundius, T. (2016). *Spectrochim. Acta A Mol. Biomol. Spectrosc.* **153**, 625–636.
Westrip, S. P. (2010). *J. Appl. Cryst.* **43**, 920–925.

supporting information

Acta Cryst. (2025). E**81**, 252-256 [https://doi.org/10.1107/S2056989025001379]

Synthesis, crystal structure, Hirshfeld surface and crystal void analysis of 4-fluorobenzo[*c*][1,2,5]selenadiazol-1-ium chloride

Atash V. Gurbanov, Tuncer Hökelek, Gunay Z. Mammadova, Khudayar I. Hasanov, Tahir A. Javadzade and Alebel N. Belay

Computing details

4-Fluorobenzo[*c*][1,2,5]selenadiazol-1-ium chloride

Crystal data

$C_6H_4FN_2Se^+\cdot Cl^-$
$M_r = 237.52$
Monoclinic, $P2_1/c$
$a = 6.889$ (4) Å
$b = 7.250$ (5) Å
$c = 15.183$ (10) Å
$\beta = 90.90$ (3)°
$V = 758.2$ (9) Å^3
$Z = 4$
$F(000) = 456$
$D_x = 2.081$ Mg m^{-3}
Mo $K\alpha$ radiation, $\lambda = 0.71073$ Å
Cell parameters from 3456 reflections
$\theta = 3.0$–27.8°
$\mu = 5.25$ mm^{-1}
$T = 296$ K
Plate, yellow
0.34 × 0.23 × 0.14 mm

Data collection

Bruker APEXII CCD diffractometer
φ and ω scans
Absorption correction: multi-scan (SADABS; Krause *et al.*, 2015)
$T_{min} = 0.252$, $T_{max} = 0.498$
9806 measured reflections
1768 independent reflections
1528 reflections with $I > 2\sigma(I)$
$R_{int} = 0.046$
$\theta_{max} = 27.9°$, $\theta_{min} = 3.0°$
$h = -8\rightarrow9$
$k = -8\rightarrow9$
$l = -19\rightarrow19$

Refinement

Refinement on F^2
Least-squares matrix: full
$R[F^2 > 2\sigma(F^2)] = 0.025$
$wR(F^2) = 0.055$
$S = 1.07$
1768 reflections
100 parameters
0 restraints
Primary atom site location: structure-invariant direct methods
Secondary atom site location: difference Fourier map
Hydrogen site location: mixed
H-atom parameters constrained
$w = 1/[\sigma^2(F_o^2) + (0.0085P)^2 + 0.4749P]$ where $P = (F_o^2 + 2F_c^2)/3$
$(\Delta/\sigma)_{max} = 0.001$
$\Delta\rho_{max} = 0.27$ e Å^{-3}
$\Delta\rho_{min} = -0.41$ e Å^{-3}

Special details

Geometry. All esds (except the esd in the dihedral angle between two l.s. planes) are estimated using the full covariance matrix. The cell esds are taken into account individually in the estimation of esds in distances, angles and torsion angles; correlations between esds in cell parameters are only used when they are defined by crystal symmetry. An approximate (isotropic) treatment of cell esds is used for estimating esds involving l.s. planes.

Fractional atomic coordinates and isotropic or equivalent isotropic displacement parameters (Å²)

	x	*y*	*z*	U_{iso}*/U_{eq}
Se1	0.22554 (3)	0.60768 (4)	0.44282 (2)	0.03658 (9)
Cl1	0.10964 (9)	0.22691 (9)	0.45729 (5)	0.04730 (16)
F1	0.7896 (2)	0.5196 (3)	0.29631 (12)	0.0683 (5)
N1	0.4403 (3)	0.5410 (3)	0.38754 (13)	0.0369 (4)
N2	0.2954 (3)	0.8495 (3)	0.42793 (13)	0.0369 (4)
H2N	0.224535	0.941205	0.440922	0.044*
C1	0.5393 (3)	0.6891 (4)	0.36440 (14)	0.0341 (5)
C2	0.4619 (3)	0.8681 (3)	0.38569 (14)	0.0345 (5)
C3	0.5575 (3)	1.0345 (4)	0.36309 (16)	0.0430 (6)
H3	0.506553	1.149204	0.377483	0.052*
C4	0.7274 (4)	1.0179 (5)	0.31933 (17)	0.0502 (7)
H4	0.794289	1.124494	0.304325	0.060*
C5	0.8070 (4)	0.8445 (5)	0.29559 (18)	0.0521 (7)
H5	0.922383	0.840209	0.264667	0.063*
C6	0.7178 (3)	0.6873 (4)	0.31723 (16)	0.0434 (6)

Atomic displacement parameters (Å²)

	U^{11}	U^{22}	U^{33}	U^{12}	U^{13}	U^{23}
Se1	0.03476 (13)	0.02831 (14)	0.04693 (14)	0.00279 (9)	0.00965 (8)	−0.00143 (11)
Cl1	0.0487 (3)	0.0279 (3)	0.0659 (4)	0.0022 (2)	0.0187 (3)	−0.0004 (3)
F1	0.0536 (9)	0.0656 (14)	0.0865 (12)	0.0207 (9)	0.0249 (8)	−0.0028 (11)
N1	0.0354 (9)	0.0326 (12)	0.0427 (10)	0.0062 (8)	0.0051 (8)	−0.0022 (9)
N2	0.0378 (9)	0.0262 (12)	0.0469 (11)	0.0033 (8)	0.0091 (8)	−0.0032 (9)
C1	0.0312 (10)	0.0345 (14)	0.0367 (11)	0.0027 (9)	0.0008 (8)	−0.0027 (10)
C2	0.0354 (11)	0.0332 (14)	0.0347 (11)	−0.0019 (9)	−0.0008 (8)	−0.0001 (10)
C3	0.0460 (12)	0.0352 (15)	0.0477 (13)	−0.0055 (11)	−0.0009 (10)	0.0023 (12)
C4	0.0463 (13)	0.053 (2)	0.0509 (15)	−0.0145 (12)	0.0026 (11)	0.0094 (13)
C5	0.0367 (12)	0.066 (2)	0.0536 (15)	−0.0020 (12)	0.0100 (10)	0.0076 (15)
C6	0.0359 (11)	0.0482 (18)	0.0462 (14)	0.0078 (11)	0.0066 (10)	−0.0006 (12)

Geometric parameters (Å, º)

Se1—N1	1.779 (2)	C2—C3	1.419 (4)
Se1—N2	1.833 (2)	C3—C4	1.360 (4)
F1—C6	1.352 (4)	C3—H3	0.9300
N1—C1	1.322 (3)	C4—C5	1.420 (5)
N2—C2	1.330 (3)	C4—H4	0.9300
N2—H2N	0.8500	C5—C6	1.339 (4)

C1—C6	1.433 (3)	C5—H5	0.9300
C1—C2	1.442 (4)		
N2···Cl1^{i}	3.056 (3)	F1···N1	2.800 (3)
H2N···Cl1^{i}	2.23	H5···F1^{ii}	2.56
N1—Se1—N2	88.83 (10)	C4—C3—H3	121.7
C1—N1—Se1	109.94 (18)	C2—C3—H3	121.7
C2—N2—Se1	112.75 (17)	C3—C4—C5	122.8 (3)
C2—N2—H2N	122.4	C3—C4—H4	118.6
Se1—N2—H2N	124.5	C5—C4—H4	118.6
N1—C1—C6	125.1 (2)	C6—C5—C4	120.7 (2)
N1—C1—C2	118.5 (2)	C6—C5—H5	119.6
C6—C1—C2	116.3 (2)	C4—C5—H5	119.6
N2—C2—C3	127.6 (2)	C5—C6—F1	122.5 (2)
N2—C2—C1	110.0 (2)	C5—C6—C1	121.1 (3)
C3—C2—C1	122.5 (2)	F1—C6—C1	116.5 (3)
C4—C3—C2	116.7 (3)		
N2—Se1—N1—C1	0.14 (16)	N2—C2—C3—C4	−179.8 (2)
N1—Se1—N2—C2	0.13 (17)	C1—C2—C3—C4	0.4 (3)
Se1—N1—C1—C6	−178.75 (19)	C2—C3—C4—C5	0.8 (4)
Se1—N1—C1—C2	−0.4 (3)	C3—C4—C5—C6	−1.2 (4)
Se1—N2—C2—C3	179.83 (19)	C4—C5—C6—F1	−179.6 (2)
Se1—N2—C2—C1	−0.3 (2)	C4—C5—C6—C1	0.4 (4)
N1—C1—C2—N2	0.5 (3)	N1—C1—C6—C5	179.2 (2)
C6—C1—C2—N2	179.0 (2)	C2—C1—C6—C5	0.8 (4)
N1—C1—C2—C3	−179.7 (2)	N1—C1—C6—F1	−0.9 (4)
C6—C1—C2—C3	−1.2 (3)	C2—C1—C6—F1	−179.31 (19)

Symmetry codes: (i) *x*, *y*+1, *z*; (ii) −*x*+2, *y*+1/2, −*z*+1/2.

Hydrogen-bond geometry (Å, º)

D—H···*A*	*D*—H	H···*A*	*D*···*A*	*D*—H···*A*
N2—H2*N*···Cl1^{i}	0.85	2.23	3.056 (3)	163

Symmetry code: (i) *x*, *y*+1, *z*.